Article

Not peer-reviewed version

Study on Rock Strata Movement Deformation and Surface Subsidence in Mining Area Based on PS-InSAR Technology

Xuxing Huang , Xuefeng Li * , Hequn Li , Yihao Yang , Shanda Duan , Wuning Xiao , Han Du , Hao Liu

Posted Date: 30 June 2023

doi: 10.20944/preprints202306.2212.v1

Keywords: PS-InSAR; Goaf management; Surface subsidence; rock strata movement deformation

Article

Study on Rock Strata Movement Deformation and Surface Subsidence in Mining Area Based on PS-InSAR Technology

Xuxing Huang [1], Xuefeng Li [1,*], Hequn Li [1], Yihao Yang [1], Shanda Duan [1], Wuning Xiao [1], Han Du [1] and Hao Liu [1]

[1] College of Resources, Environment and Materials, Guangxi University, Nanning 530000, China
* Correspondence: 757092393@qq.com; Tel.: +8613768373489

Abstract: The rock strata movement deformation generated by the mining process of the mine will inevitably lead to surface subsidence and a series of environmental hazards, so it is particularly important to monitor the rock strata movement deformation and surface subsidence in the goaf area. With the development of surface subsidence monitoring technology, InSAR technology has been widely used in the research of surface subsidence in mining areas with the advantages of high precision and wide monitoring. In this paper, by obtaining the image data of 59 Sentinel-1A scenes in the mining area, the obtained PS points were analyzed and processed by ArcGIS difference analysis by PS-InSAR technology, and the surface deformation cloud map and settlement curve of the mining area in various periods were obtained, and the rock strata movement deformation and surface subsidence law of the goaf before treatment and after different treatment methods were studied by influencing factors such as stope layout and mining depth. The results show that the rock strata movement deformation and surface subsidence degree of the goaf under different treatment methods are different due to different influencing factors, and their positions also change dynamically with time. Applying InSAR technology to study rock strata movement deformation and surface subsidence can provide an important basis for mine safety mining, goaf treatment, rock strata movement deformation and surface subsidence monitoring.

Keywords: PS-InSAR; Goaf management; Surface subsidence; rock strata movement deformation

1. Introduction

According to statistics, the land damaged by mining activities in China has exceeded 4 million hm^2, of which more than 1.4 million hm^2 and the area of surface collapse is more than 35.2hm^2 caused by mining activities[1], The main cause of ground damage and collapse is due to the formation of a mining area as a result of ore extraction, which breaks the original rock stress balance and causes rock movement deformation in the rock stress redistribution[2]. Generally, the movement deformation of underground mining rock mass are divided into two stages, and the surface will produce four settlement areas[3], In the initial stage of mining, the horizontal in-situ stress is not completely released, the geological structure has less influence on the surface subsidence[4], and when the exposed area of the goaf reaches a certain value, there is a sudden process of rock strata movement deformation, resulting in surface subsidence[5,6], and the rock strata movement deformation and surface subsidence law under different working conditions are different[7–11]; Therefore, in order to ensure safe and efficient mining of mines, it is indispensable to study the movement deformation and surface subsidence monitoring of mine rock masses.

With the development of science and technology, surface deformation characterization is increasing, and InSAR monitoring technology has the advantages of low cost, high precision and wide monitoring compared with traditional monitoring. It is widely used in surface subsidence, landslide and other monitoring[12–16]. Given the surface subsidence in the mining area, Yao J. et al. concluded that surface settlement is a lagged representation of the effects of deep rock deformation and rupture to the surface by InS AR observations and ground fracture dynamics[17]. Du D et al.

used the PS-InSAR technique to monitor ground subsidence in an area, [and] the integrated hydrogeological situation was analyzed and described, providing a new idea for surface subsidence monitoring [18]; Yang, W et al. used InSAR to obtain surface subsidence information and analyzed the surface subsidence mechanism regarding the human-machine relationship, geological faults, and lithological structures. The results indicate that the human-machine relationship is the main cause of surface deformation, and faults and lithological formations are the controlling factors of surface subsidence[19].

Therefore, the goaf filling treatment is one of the effective means to ensure mining safety, control the movement deformation of rock mass, and avoid surface collapse[20]. However, most of the rock strata movement deformation and surface subsidence of mine filling and mining are studied by theoretical formulas, similar materials, and numerical simulation combined with traditional monitoring methods[7,21–23]. However, the rock strata movement, deformation, and surface subsidence are affected by various factors, resulting in different degrees and locations of influence in each period. In addition, due to the limitations of traditional monitoring methods, it cannot reflect the complete process of rock strata movement deformation and surface subsidence before and after goaf treatment. Therefore, this study takes the goaf area of the west wing of Taibao in Guiping City, Guangxi Province, as an example, uses PS-InSAR technology to obtain surface subsidence information from 2015 to 2021, clarifies the temporal and spatial distribution characteristics of surface subsidence in mining areas, compares and verifies by using the level monitoring data in the same period, and takes the state and governance mode of the goaf as the influencing factors to explore the evolution process of rock strata movement and settlement under different treatment modes in the goaf area and the changing trend of surface subsidence under different treatment periods.

2. Materials and Methods

2.1. The Study Region

The Taibao tin-based pit mining area is next to Daxu Town in Guigang City and Shilong Town in Guiping City. The topography is gentle, with a ground elevation ranging from 39.8 to 42.5m. The overall terrain is slightly lower in the northeast and higher in the southwest, with the surface covered by a Quaternary soil layer. The surrounding area of the mining area consists mainly of farmland and some scattered residential areas. Nine ore bodies are distributed in the west and east wings of the mining area, with deposit heights ranging from +40m to -100m and an inclination of approximately 20°. The mine uses a combination of open pit and underground mining methods to extract the ore body. The open pit mines the ore body between +20m and +40m elevation. In comparison, the underground employs a trackless ramp road comprehensive mining method to extract the ore body between -80m and 0m.

Recently, the mine has mainly mined the ore body in the west wing. The goaf in the west wing mainly exists within lines 11 to 23 at 0-25m elevations. In January 2018, the goaf in the west wing was treated. The treatment plan is shown in **(b-g)**: reinforcement of unstable ore pillars in goafs 1 and 5; closure and isolation treatment of goafs 2 and 4; overall waste rock mortar filling of goaf 3; closure and isolation and partial filling reinforcement of goaf 6. The treatment was completed in March 2019.

2.2. Data

The area studied is the goaf on the west wing of the mine, and the distribution is shown in **a**. In order to monitor the surface deformation of the mine goaf before and after treatment, the Sentinel-1A image of Decending VV polarization was selected as the data source, and the image data of the mining area was selected before, during, one year and the second year after the goaf treatment, the image acquisition time was as follows:

 doi:10.20944/preprints202306.2212.v1

1. 21 images from June 2015 to January 2018 before the Goaf treatment;
2. 15 images from January 2018 to March 2019 during the Goaf governance period;
3. 13 images from March 2019 to March 2020 in the year after Goaf remediation;
4. 13 images from March 2020 to March 2021 in the second year after Goaf remediation.

At the same time, the precision orbit information of the same period was selected to correct it, and the DEM data with a resolution of 30m STRM1_V3 NASA was selected to remove the terrain residuals. The image acquisition time and related information for each period are shown in Appendix **Error! Reference source not found.**.

Figure 1. Goaf distribution and treatment plan map. (a) The scope of the mining area and the surface optical image of the mine area; (b) The distribution and management of the roof and pillar of the No. 1 mining area; (c) The distribution and management of the roof and pillar of No. 2 mining area; (d) The distribution and management of the roof and pillar of No. 3 mining area; (e) The distribution and management of the roof and pillar of No. 4 mining area; (f) The distribution and management of the roof and pillar of No. 5 mining area; (g) The distribution and management of the roof and Pillar No. 6 mining area.

2.3. Principle of PS-InSAR technology

The basic principle of PS-InSAR technology is to track ground objects through the interaction between electromagnetic waves emitted by the space station's radar and targets, which need to be targeted with stable scattering characteristics in time and space, such as buildings, bare rock, Etc. These targets with stable scattering characteristics and high coherence greatly reduce the influence of noise and coherence on monitoring in phase space due to their small influence by space and time. PS-InSAR technology solves the problems of the long monitoring cycle of traditional technology,

Preprints (www.preprints.org) | NOT PEER-REVIEWED | Posted: 30 June 2023 doi:10.20944/preprints202306.2212.v1

slow engineering speed, great influence by natural weather conditions, and large limitation of monitoring scope.

N interferograms are obtained by processing N+1 image data of the study area, and the corresponding differential interferograms are obtained after differential DEM processing. Then the phase of the Nth interferogram element is $\Delta\varphi = \frac{4\pi}{\lambda} R_n$, The differential phase can be expressed as[24]:

$$\varphi_n = \frac{4\pi}{\lambda R_n \bullet \sin\theta} B^n{}_{\perp} \delta_H + \frac{4\pi \bullet \cos\theta}{\lambda} h + \varphi_A^n + \xi^n \quad (1)$$

where R_n is the oblique distance from the sensor to the ground target; θ is the radar angle of incidence; λ is the radar wavelength; $B^n{}_{\perp}$ is the effective spatial baseline; δ_H is the elevation correction value; h is the amount of surface settlement; φ_A^n is the atmospheric phase; ξ^n is the noise phase.

In order to attenuate the effect of the atmospheric phase, the interferometric phase of adjacent PS points can be differenced again from the spatial scale, then the phases of PS points i, j, respectively, as:

$$\begin{cases} \varphi_n^i = a^i B^n{}_{\perp} \delta_H^i + b^i t^n v + \varphi_{n-res}^i \\ \varphi_n^j = a^i B^n{}_{\perp} \delta_H^j + b^j t^n v + \varphi_{n-res}^j \end{cases} \quad (2)$$

Differentiating the two equations again gives the PS point phase difference equation as:

$$\Delta\varphi_n = aB^n{}_{\perp} \Delta\delta_H + b_1 t^n v + \Delta\varphi_{n-res} \quad (3)$$

If the difference in settlement velocity Δv and the elevation correction $\Delta\delta_H$ between two adjacent PS points can be correctly estimated, and $\varphi_{n-res} < \pi$, the complete phase difference $\Delta\varphi_n$ between the two points can be found and the gradient of $\Delta\varphi_n$ can be regarded as the gradient of φ_n. If the complete value of the gradient is known, φ_n v can be solved and the deformation value of the surface can be found in turn.

2.4. Data processing processes

The PS-InSAR data processing steps consist of the following five main parts[25]: selection of the common master image, differential interference processing, selection of PS candidate points, removal of atmospheric phases and finally, the deformation results.

1. A large number of SAR images are compared and interfered with in order of data, taking into account temporal and spatial baseline thresholds, as well as time nodes, meteorological conditions and Doppler mass frequencies, Etc., to select the super master image.
2. Differential interference processing of the super master image using DEM data.
3. The PS points with high signal-to-noise ratio and high coherence characteristics are selected, the interferometric phase of these target points is processed, and the Delonet network function model is used to analyse and remove the delay fluctuations caused by the signal propagation process.
4. Finally, the function model $Disp = K + V * (t - t_0)$ is used to estimate the atmospheric residuals, the linear phase residuals of the flat-earth phase and the deconvolution process, Etc., and then two atmospheric filters with different fluxes of high pass and low pass are used for atmospheric correction using the time window of 365 days and the spatial window of 1.2Km respectively. the result is the final deformation result of the PS-inSAR technique.

Preprints (www.preprints.org) | NOT PEER-REVIEWED | Posted: 30 June 2023 doi:10.20944/preprints202306.2212.v1

5. The resulting vector file of deformation results is flexibly time-series superimposed on the satellite image to visualise the point information, and interpolation is used to generate a subsidence cloud map to visualise the subsidence results.

3. Results and Analysis

3.1. PS-InSAR monitoring result

The radar images of each period were processed by the above process to obtain 3,395 PS points in the first period finally, 47,13 PS points in the second period, 5,789 PS points in the third period, and 4,377 PS points in the fourth period.The distribution of PS points for each period is shown in **Error! Reference source not found.**, where red represents sinking points and green represents rising p oints.

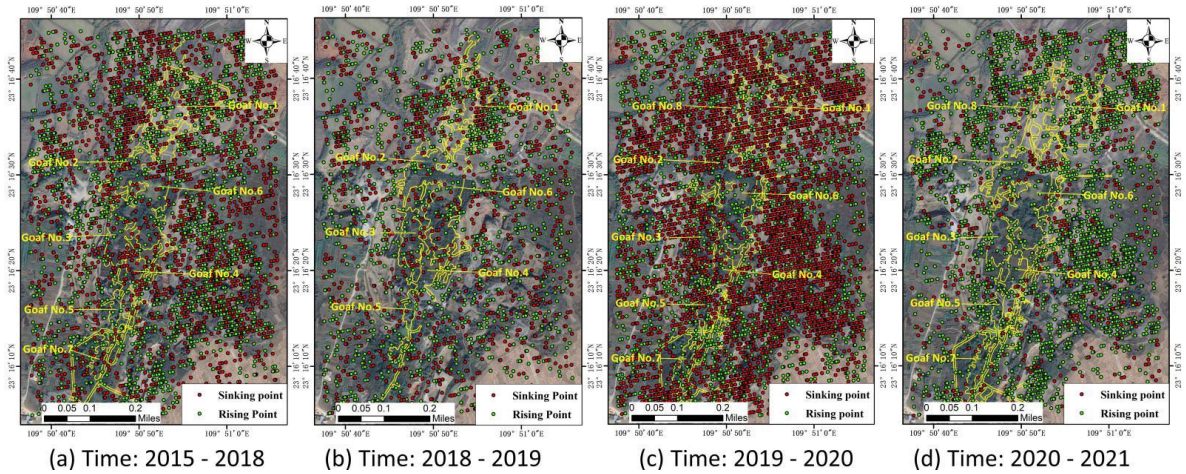

Figure 2. Distribution of PS points by time period. (a) PS point distribution map before the treatment of the mining area; (b) PS point distribution map during the treatment of the mining area; (c) PS point distribution map for one year after the treatment of the mining area; (d) PS point distribution map for the second year after the treatment of the mining area.

3.2. PS point accuracy verification

In order to ensure the accuracy and reliability of the monitoring results, the proximity method is used to compare the level point measurement data with the mean value of the adjacent PS point to verify the monitoring accuracy[26]. According to the acquisition time of radar data images, combined with the level measurement data of the mine, the PS-InSAR deformation data from March 2019 to March 2020 was finally tested by the level point data of the mine area, and the error value after comparison is shown in **Error! Reference source not found.**. The deformation rates and errors for e ach monitoring point are shown in Appendix **Error! Reference source not found.**.

Preprints (www.preprints.org) | NOT PEER-REVIEWED | Posted: 30 June 2023 doi:10.20944/preprints202306.2212.v1

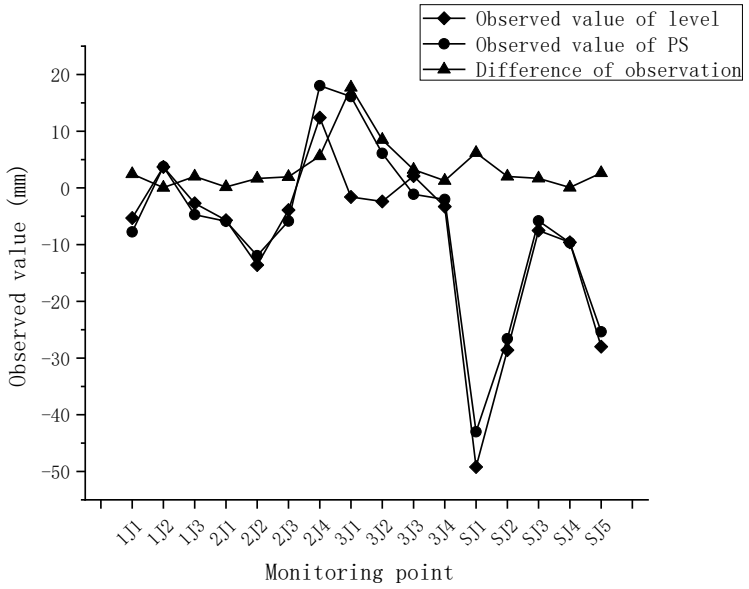

Figure 3. Monitoring accuracy verification.

From the **Error! Reference source not found.**, it can be concluded that the error value of point 3 J1 is more prominent than other error values, because this point is at the three-way intersection. The mine car passing through produces dust and falling debris causing slight lifting of the road surface, resulting in a positive PS deformation value, while the level point is less affected by the mine car at the roadside, except for point 3J1, the absolute minimum error of the level point and PS point is 8.5mm, the minimum absolute error is 0.046mm. The mean square difference is 2.4mm, so it can be proved that PS-InSAR is feasible to monitor the surface deformation in the mine area.

3.3. Surface Subsidence Analysis

The resulting PS points were processed by ArcGIS differential analysis to obtain a cloud map of the mine deformation distribution, as shown in **Error! Reference source not found.**.

Figure 4. Surface subsidence map of the extraction area by period. (a) surface subsidence map before the treatment of the mining area; (b) surface subsidence map during the treatment of the mining area; (c) surface subsidence map for one year after the treatment of the mining area; (d) surface subsidence map for the second year after the treatment of the mining area.

The movement deformation of rock formations caused by mining is a process that has a comprehensive influence of many factors, which is affected by the hydrogeological conditions,

Preprints (www.preprints.org) | NOT PEER-REVIEWED | Posted: 30 June 2023 doi:10.20944/preprints202306.2212.v1

geological engineering conditions, mining depth, stope layout, and different governance methods of the goaf in the mining area[27–30]. According to the actual situation of the mine, the rock strata movement and surface subsidence laws of three different treatment methods: goaf No. 3 (full filling), goaf No. 6 (partial filling) and goaf No. 2 (closed goaf), were studied according to the actual situation of the mine.

3.3.1. Surface subsidence law before goaf is not filled.

In the mining process, the layout of the stope, such as the mining height, the size of the ore column, and the layout position, directly affect the stability of the goaf. From

above, it can be seen that before the treatment of some goaves, due to the unreasonable layout parameters in the mining process, the stress concentration of the ore column and the roof plate was caused, resulting in an unstable roof and unstable part of the ore pillar in the No. 3 goaf area, unstable ore pillars and roof in the northern, central and southern parts of the No. 6 goaf area, and only one more column in the No. 2 goaf area was unstable. Therefore, it can be seen in **Error! Reference source n ot found.**(a) that the No. 3 goaf area is as a whole, the northern, central and southern areas of the No. 6 goaf area can be seen in **Error! Reference source not found.**(b), and the settlement amount at the unstable ore pillar area of the No. 2 goaf area is large in **Error! Reference source not found.**(c), so the rock strata movement deformation in these areas are strong.

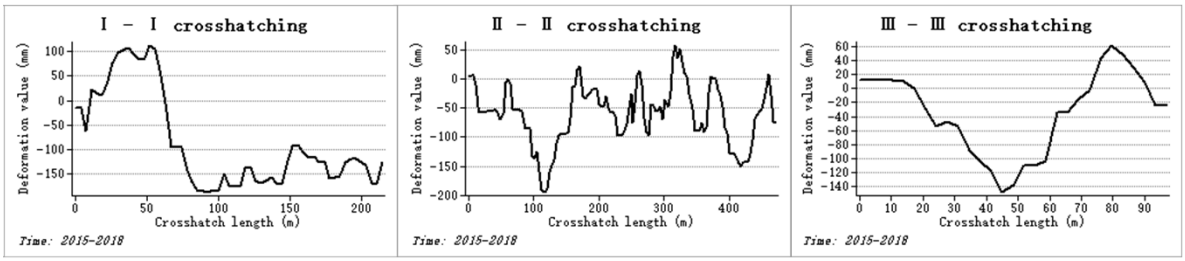

(a) (b) (c)

Figure 5. Surface subsidence curve before the treatment of the mining area. (a) Surface subsidence curve before the treatment of No. 3 mining area; (b) Surface subsidence curve before the treatment of No. 6 mining area; (c) Surface subsidence curve before the treatment of No. 2 mining area.

The mining depth of the ore body determines the size of the top plate bearing the load of the overlying rock layer, which is the key factor affecting the sinkage of the top plate in the mining area, combined with the analysis of the profile of each mining area, **Error! Reference source not found.**. it c an be seen that the smaller the overlying load, the smoother the settlement curve; the sinkage of the top plate rock layer increases with the increase of the mining depth, and the maximum value of the settlement is approximately the same as the maximum position of the mining depth, but not the same, part of the settlement value at the unstable top plate is also larger due to the unreasonable placement of the ore column causing the top plate to bear a larger overlying load, which is generally consistent with the actual.

Preprints (www.preprints.org) | NOT PEER-REVIEWED | Posted: 30 June 2023 doi:10.20944/preprints202306.2212.v1

Figure 6. Section view of mining area.

3.3.2. Surface subsidence law during the filling of the mining area

Filling management of the mining area controls the movement deformation of the rock mass and prevents the surface from caving in. The effect of different filling materials and filling rates to control rock movement deformation is also different[31].

Because the roof plate and ore column of the No. 3 goaf area are unstable, it is necessary to carry out all filling treatments of the goaf, with the increase of filling rate during the filling process. However, the filling body has a supporting effect on the unstable ore column and surrounding rock; to a certain extent, the movement deformation of the rock mass are controlled. However, the surface subsidence at this stage is not much different from before treatment; on the one hand, it is determined by the mechanical characteristics of the filling body; the stronger the compression resistance of the filling body, the stronger the support force for the ore column, and the slower the movement deformation speed of the rock mass; On the other hand, the filling rate determines it, the higher the filling rate, the smaller the empty ceiling, and the smaller the surface subsidence after filling[32–35]. Therefore, it can be seen from **Error! Reference source not found.**(a) that the surface subsidence of g oaf No. 3 during the full-filling treatment period has been slightly slowed, but the degree of mitigation is small due to the unstable roof and ore pillars in the goaf. On the one hand, because the filling material is related to the strength of the filling body, on the other hand, there is a certain empty roof height after all filling. The empty area's roof plate and ore column still provide the main source of supporting pressure, so the control of the unstable rock strata movement deformation of the roof plate and ore column in the goaf is limited, so it still maintains a large settlement value. In addition, it can be seen from the figure that the centre of the settlement area moves to the depth of the No. 3 goaf. The settlement at the maximum mining depth is 150.9mm, which is significantly greater than the settlement amount in other areas because, due to the influence of the mining depth, the larger the mining depth, the greater the load of the overlying rock layer, and the greater the compression of the filler, resulting in a large settlement in the mining depth is greater than that in the shallow part. Therefore, during the full-filling treatment, the rock mass in the shallow part of the mining depth has a large degree of movement deformation.

Preprints (www.preprints.org) | NOT PEER-REVIEWED | Posted: 30 June 2023 doi:10.20944/preprints202306.2212.v1

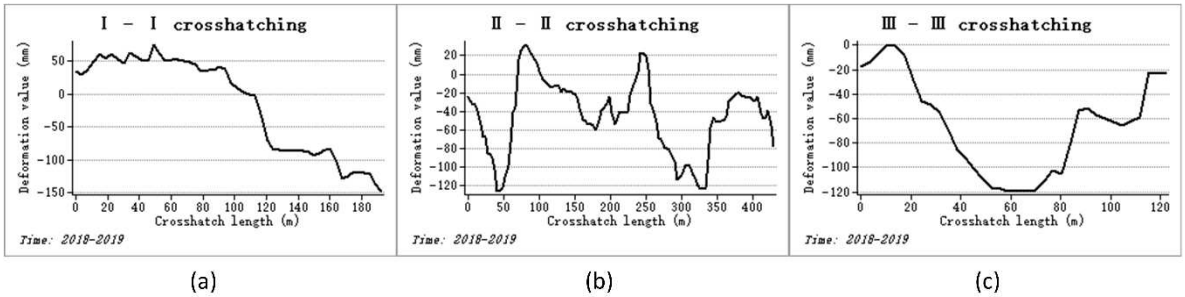

Figure 7. Surface subsidence curve during the treatment of the mining area. (a) Surface subsidence curve during the treatment of No. 3 mining area; (b) Surface subsidence curve during the treatment of No. 6 mining area; (c) Surface subsidence curve during the treatment of No. 2 mining area.

Due to the unstable local roof and ore column of the No. 6 goaf, the unstable area of the local filling goaf was used for treatment. Building a closed wall in filling and treatment is equivalent to providing a fulcrum for the roof rock layer, reducing the compressive stress and roof tension failure supported by the ore column, and protecting the ore column. However, in the form of a cantilever beam in the unfilled area, the rock strata movement deformation is "inverted trapezoidal" sinking [ref], so the vertical displacement of the roof plate in the filling area of the working face gradually slows down, and the vertical displacement of the roof in the unfilled area increases with the inclination direction of the rock layer[36,37]. Therefore, it can be seen from **Error! Reference source not found.**(b) that the surface subsidence of the No. 6 goaf gradually attenuated during the local filling treatment, but the settlement in the untreated area increased to varying degrees. The settlement value at the northern end increased by 58.12mm compared with before treatment, and the settlement value at the southern end increased by 31.5mm compared with before treatment. It can be concluded that the degree of rock strata movement deformation in the untreated area during the local filling treatment period is greater than that in the treated area.

By comparing and analyzing the variation characteristics of vertical displacement of closed goaf and local filling roofs, the vertical displacement trend of the two roofs is similar, and the vertical displacement of the direct roof is not much different in the unfilled area. Therefore, **Error! Reference source not found.**(c) shows that the surface of the No. 2 goaf is still sinking greatly during the closed goaf, the rock strata movement deformation are still in the unstable area, and the settlement funnel is concentrated at the unstable ore column. The maximum settlement in the figure is 118.9mm, indicating that the time required for the rock mass stress redistribution to equilibrium is longer under the closed treatment of the goaf area, resulting in a longer duration of rock mass movement, so the rock strata movement and is still in the area where the unstable ore column is located.

3.3.3. Surface subsidence law in the first year after the treatment of the mining area

From **Error! Reference source not found.**(a), it can be concluded that the No. 3 Goaf in the first year after full filling treatment with the compression of the filling body, the height of the empty roof gradually decreases; at this time, the load of the overlying rock layer is mainly borne by the filling body, roof plate and ore column, which restricts the movement of the rock mass to a certain extent[33,35], so the settlement area is significantly reduced. The surface subsidence slows down significantly, but the settlement amount at the large mining depth is still greater than the shallow part, so the settlement at the maximum mining depth in the figure is 38.3mm, greater than the settlement in other areas.

It can be seen from **Error! Reference source not found.**(b) that the surface subsidence of the No. 6 goaf area in the first year after local filling treatment gradually decays to stop. At the same time, there is still a small settlement in the unfilled area, but the impact on the surface is not large; the maximum settlement value at the southern end is 19.8mm, and the maximum settlement at the northern end is 30.9mm; the settlement area is still mainly located in the unfilled place, but the settlement centre is located at the edge of the empty area, which can be concluded that the rock strata

Preprints (www.preprints.org) | NOT PEER-REVIEWED | Posted: 30 June 2023 doi:10.20944/preprints202306.2212.v1

movement and at this time moves from the untreated area to the side of the goaf and gradually attenuates.

From **Error! Reference source not found.**(c), it can be concluded that the surface subsidence of t he No. 2 goaf area in the first year after closure and treatment has been greatly slowed down, and there is still a slight settlement at the roof of the unstable ore column, indicating that the stress redistribution of the rock mass has gradually reached equilibrium and the rock strata movement and has gradually weakened. In addition, there is still a large settlement in the northern part of the No. 2 empty area, and the maximum settlement value of the goaf is 34.2mm because the ore body in the northern part of the mining area in the 19-20 mining season leads to the activation of the upper overlying rock layer under the influence of mining.

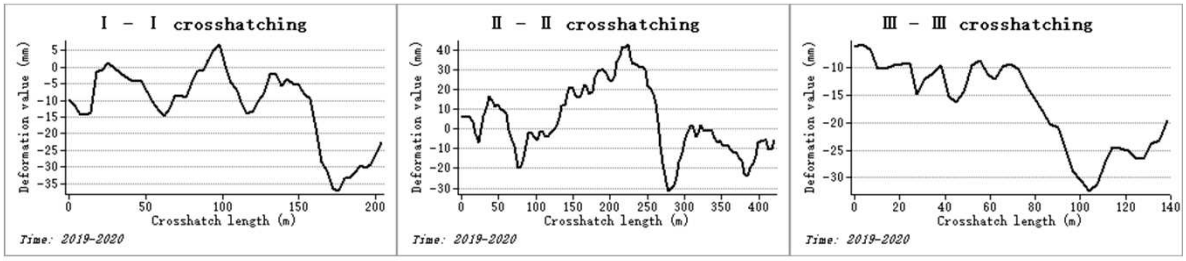

Figure 8. Surface sedimentation curve in the first year of completion of mining area treatment. (a) surface subsidence curve of the No. 3 mining area after one year of treatment; (b) surface subsidence curve of the No. 6 mining area after one year of treatment; (c) surface subsidence curve of the No. 2 mining area after one year of treatment.

3.3.4. Surface subsidence law in the second year after the treatment of the mining area

From **Error! Reference source not found.**, it can be concluded that in the second year after the t reatment of goaf No. 3, No. 6 goaf and No. 2 goaf area, the rock strata movement tends to stop, the surface subsidence stops, and most areas cause the surface to rise due to the influence of engineering activities. Only the northern part of goaf No. 2 is still sinking due to the influence of mining, and the maximum settlement value of point D3 is 13.4mm, but overall the surface subsidence shows a trend of attenuation to stop.

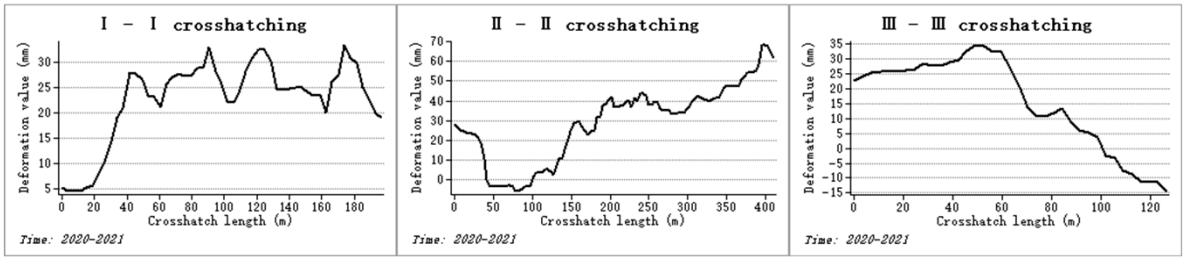

Figure 9. Surface sedimentation curve in the second year after the completion of mining area treatment. (a) Surface subsidence curve of the second year after the completion of the treatment of No. 3 mining area; (b) Surface subsidence curve of the second year after the completion of the treatment of No. 6 mining area; (c) Surface subsidence curve of the second year after the completion of the treatment of No. 2 mining area.

4. Discussion

The rock mass law obtained by analyzing the surface subsidence cloud map and the settlement curve of each goaf by three different management methods of goaf is as follows: rock strata movement deformation and surface subsidence law of all filled goaf area[34,35,37,38]: the rock strata movement and in the goaf area before the treatment is distributed in the unstable area, and the rock

strata movement and in the goaf as a whole is severe, and the surface subsidence caused by it is large, and the surface subsidence gradually increases with the increase of the overlying load. During the full filling treatment of the goaf area, due to the influence of the strength of the filling body, the amount of empty roof and the depth of mining, the degree of movement deformation of the rock strata is large, and the moving deformation of the deep rock strata are greater than that in the shallow part. The surface subsidence is slowed down, and the degree of slowdown is greater in the shallow mining depth than in the large mining depth. In the first year after treatment, rock strata movement deformation intensity was greatly reduced and gradually stabilized. However, the rock strata movement deformation in the deep part was still larger than that in the shallow part, and the surface subsidence gradually slowed down, but the surface subsidence was still greater at the large mining depth than in the shallow mining depth. In the second year after the completion of treatment, rock strata movement deformation tended to stop, and surface subsidence stopped.

Rock strata movement deformation law of local filling treatment goaf area[39–41]: The rock strata movement deformation is distributed in unstable areas when the goaf area is not treated, and the rock strata movement deformation in the northern, central and southern areas of the goaf area is violently deformed, resulting in large surface subsidence, and the surface subsidence gradually increases with the increase of mining depth. When the goaf is gradually weakened, and the surface subsidence is gradually slowed down due to the establishment of a closed wall in the local filling treatment period, the rock strata movement deformation and surface subsidence in the untreated area increase. In the first year after treatment, rock strata movement deformation intensity was greatly reduced and gradually stabilized, and surface subsidence was controlled. However, the rock strata movement, deformation, and surface subsidence in the untreated area were larger than in the treated area. In the second year after the completion of treatment, overburden movement stops, and surface subsidence stops.

Rock strata movement deformation law in closed goaf area[6,9,42]: When the goaf is not closed for treatment, the rock strata movement deformation is distributed in the position of an unstable ore column, and the rock mass moves violently and causes large surface subsidence. When the goaf takes a long time to redistribute the rock mass stress to equilibrium during the closed treatment period, the rock strata movement deformation are still in the area where the unstable ore column is located. The surface maintains a large settlement, and the intensity of rock strata movement deformation is greatly slowed down and gradually stabilized in the first year after the completion of closed treatment, and the surface subsidence is controlled, but it is still in the area where the unstable ore column is located. In the second year after closed treatment was completed, overburden movement stopped, and surface subsidence stopped.

5. Conclusions

In this paper, a PS-InSAR technology is proposed to monitor the surface subsidence cloud map and surface subsidence curve of the mining area at each stage of goaf treatment and study the law of rock strata movement deformation and surface subsidence from underground mining to treatment, which provides a basis for safe mining, goaf treatment, rock movement and surface subsidence, and the main results are as follows:

1. According to the actual mining time of the mine, satellite images of different periods of the mining area are obtained, the PS point deformation information of the mine area is obtained by ENVI+Scrape software processing, and the surface deformation cloud map and surface subsidence curve of the mine area obtained by kriging difference processing have a small error value compared with the level measurement results of the mining area, which is consistent with the actual project, and can accurately characterize the surface deformation.
2. The surface subsidence curve obtained was analyzed, which was consistent with the on-site measurement and relevant reference results, indicating that the monitoring results were good, in line with the movement deformation of the mine rock strata and the influence of different factors such as mining parameters and mining depth was considered in the result analysis. It was concluded that the unreasonable layout of the stope in the goaf before treatment led to the

 doi:10.20944/preprints202306.2212.v1

instability of the roof, and the ore column was the main factor of surface subsidence, and the surface subsidence during the treatment period was mainly affected by the mining depth and filling materials. Therefore, this technique can reflect the rock strata movement deformation and surface subsidence characteristics of the mining area.

3. In addition, compared with the theoretical model and numerical model, the use of PS-InSAR monitoring can accurately reflect the process of rock strata movement deformation and surface subsidence in each stage from the goaf untreated, the treatment is completed, and the location of rock strata movement deformation and surface subsidence under different treatment methods in the goaf area, from the comparison of the surface subsidence curve and the actual situation of the surface of the mining area, the obtained rock strata movement deformation and surface subsidence position are in line with the actual situation of underground mining engineering.
4. The author only studied the movement deformation and surface subsidence law of the gently inclined shallow ore body, and other mining geological conditions need to be further studied.

Author Contributions: Conceptualization, Hequn Li and Hao Liu investigation data analysis, Xuxing Huang and Xuefeng Li; Writing—original draft preparation, Shanda Duan and Yihao Yang; writing—review and editing, Han Du; visualization, Wuning Xiao; supervision, Xuxing Huang and Xuefeng. All authors have read and agreed to the published version of the manuscript.

Funding: Please add: This research was funded by the National Natural Science Foundation of China (51964003).

Institutional Review Board Statement: Not applicable.

Informed Consent Statement: Not applicable.

Data Availability Statement: The Sentinel-1 datasets can be acquired freely from Copernicus and ESA, https://search.asf.alaska.edu/#/ (accessed on 21 December 2022); Optical imagery data can be obtained from Google Maps,http://www.gditu.net/ (accessed on 19 June 2020 and 11 December 2022); Level monitoring data is obtained from Taibao.

Acknowledgments: The authors would like to thank Taibao for providing free monitoring data on the level of the mine; The authors would like to thank the Copernicus program for free access to the Sentinel-1 images processed in this analysis; The authors would also like to thank Google for providing free optical imagery data of the mine.

Conflicts of Interest: The authors declare no conflict of interest.

Appendix

Table 1. Characteristics of the satellite data used in the study.

Study period ID	Date of Acquisition (DD-MM-YYYY)	Time baseline(d)	Normal baseline(m)
2015-2018	25-06-2015	-444	-84.883
	12-08-2015	-396	13.1727
	29-09-2015	-348	33.8539
	23-10-2015	-324	32.6516
	03-01-2016	-252	-19.4715
	26-05-2016	-120	15.6077
	06-08-2016	-108	-34.0751
	23-09-2016	-60	-66.3668
	10-11-2016	-48	-20.1385
	28-12-2016	0	0
	09-01-2017	12	49.7188
	14-02-2017	48	21.0417

 doi:10.20944/preprints202306.2212.v1

	15-04-2017	108	-66.7169
	09-05-2017	132	-67.5277
	14-06-2017	168	10.0376
	08-07-2017	192	62.4211
	13-08-2017	228	-54.623
	18-09-2017	252	-12.1731
	12-10-2017	276	-73.6862
	17-11-2017	312	44.9114
	11-12-2017	336	42.8753
	04-01-2018	360	829572
2018-2019	04-01-2018	-216	-39.9495
	09-02-2018	-180	-48.6742
	05-03-2018	-156	108.632
	10-04-2018	-120	-15.5787
	04-05-2018	-96	-14.5066
	09-06-2018	-60	-26.4119
	03-07-2018	-36	33.5122
	08-08-2018	0	0
	13-09-2018	36	9.61013
	07-10-2018	60	51.9931
	12-11-2018	96	-37.9488
	06-12-2018	120	19.531
	11-01-2019	156	-11.1439
	04-02-2019	180	-15.9356
	12-03-2019	216	-32.5269
2019-2020	12-03-2019	-264	-18.1204
	05-04-2019	-240	-30.4496
	11-05-2019	-204	12.9326
2019-2020	16-06-2019	-168	79.8935
	10-07-2019	-144	38.3496
	03-08-2019	-120	56.122
	08-09-2019	-84	-47.3905
	02-10-2019	-60	-91.0679
	07-11-2019	-24	-28.1256
	01-12-2019	0	0
	06-01-2020	36	60.6799
	23-02-2020	84	34.1044
	06-03-2020	96	8.25188
2020-2021	06-03-2020	-180	-30.3446
	11-04-2020	-144	-4634055

05-05-2020	-120	9.97058
10-06-2020	-84	2.89.32
04-07-2020	-60	66.266
09-08-2020	-24	-66.2685
02-09-2020	0	0
08-10-2020	36	-133.119
25-11-2020	84	76.453
19-12-2020	118	-68.5192
12-01-2021	132	46.562
17-02-2021	168	22.8765
13-03-2021	192	2.02861

Table 2. Rate of deformation and error values at each point.

Point ID	Level point deformation rate (mm/y)	PS point Deformation rate (mm/y)	The absolute value of the error (mm)
1J1	-5.3	-7.753	2.453
1J2	3.7	3.746	0.046
1J3	-2.7	-4.729	2.029
2J1	-5.7	-5.866	0.166
2J2	-13.6	-11.947	1.653
2J3	-3.9	-5.854	1.954
2J4	12.4	18.02	5.62
3J1	-1.6	16.11	17.71
3J2	-2.4	6.106	8.506
3J3	2.1	-1.127	3.227
3J4	-3.3	-2.021	1.279
SJ1	-49.2	-43.005	6.195
SJ2	-28.6	-26.585	2.015
SJ3	-7.5	-5.806	1.694
SJ4	-9.6	-9.667	0.067
SJ5	-28	-25.374	2.626

References

1. 周际; 赵财胜; 张丽佳; 王立威; 王莉莉, 矿区土地复垦与土壤修复研究进展 %J 东北师大学报(自然科学版). **2023,** *55* (01), 151-156. http://dx.doi.org/10.16163/j.cnki.dslkxb202109220001
2. Khanal, M.; Qu, Q. D.; Zhu, Y. R.; Xie, J. L.; Zhu, W. B.; Hou, T.; Song, S. K., Characterization of Overburden Deformation and Subsidence Behavior in a Kilometer Deep Longwall Mine. *Minerals* **2022,** *12* (5). http://dx.doi.org/10.3390/min12050543
3. Zhang, C.; Fu, J. X.; Song, W. D.; Tan, Y. Y.; Kang, M. C., Study on monitoring and variation law of strata movement induced by caving mining of slowly inclined large and thick orebody. *Environmental Earth Sciences* **2021,** *80* (17). http://dx.doi.org/10.1007/s12665-021-09908-9
4. Liu, X. T.; Chen, C. X.; Xia, K. Z.; Zheng, X. W.; Wang, T. L.; Yuan, J. H., Investigation of the time-dependent strata movement behaviour caused by caving method. *Rock and Soil Mechanics* **2023,** *44* (2), 563-576. http://dx.doi.org/10.16285/j.rsm.2022.1348

5. Sun, Y. J.; Zuo, J. P.; Karakus, M.; Liu, L.; Zhou, H. W.; Yu, M. L., A New Theoretical Method to Predict Strata Movement and Surface Subsidence due to Inclined Coal Seam Mining. *Rock Mechanics and Rock Engineering* **2021,** *54* (6), 2723-2740. http://dx.doi.org/10.1007/s00603-021-02424-z
6. Yu, X.; Zhao, K.; Wang, Q.; Yan, Y. J.; Zhang, Y. J.; Wang, J. Q., Relationship between Movement Laws of the Overlaying Strata and Time Space of the Mined-Out Volume. *Geofluids* **2020,** *2020*. http://dx.doi.org/10.1155/2020/2854187
7. Zuo, J. P.; Zhou, Y. B.; Liu, G. W.; Shao, G. Y.; Shi, Y., Continuous deformation law and curvature model of rock strata in coal backfill mining. *Rock and Soil Mechanics* **2019,** *40* (3), 1097-+. http://dx.doi.org/10.16285/j.rsm.2017.1995
8. Xia, K. Z.; Chen, C. X.; Wang, T. L.; Yang, K. Y.; Zhang, C. Q., Investigation of Mining-Induced Fault Reactivation Associated with Sublevel Caving in Metal Mines. *Rock Mechanics and Rock Engineering* **2022,** *55* (10), 5953-5982. http://dx.doi.org/10.1007/s00603-022-02959-9
9. Yuan, F.; Tang, J. X.; Kong, L. R., Movement Law of Overlying Strata and Abutment Pressure Redistribution Characteristic Based on Rigid Block. *Lithosphere* **2022,** *2022* (1). http://dx.doi.org/10.2113/2022/2520477
10. Xue, Y. C.; Wu, Q. S.; Sun, D. Q., Numerical investigation on overburden migration behaviors in stope under thick magmatic rocks. *Geomechanics and Engineering* **2020,** *22* (4), 349-359. http://dx.doi.org/10.12989/gae.2020.22.4.349
11. Wang, Z. W.; Song, G. F.; Ding, K., Study on the Ground Movement in an Open-Pit Mine in the Case of Combined Surface and Underground Mining. *Advances in Materials Science and Engineering* **2020,** *2020*. http://dx.doi.org/10.1155/2020/8728653
12. Li, B.; Yang, Y.; Wang, D.; Wu, Y.; Zhang, Z., Joint InSAR technology and geological data to inverse the surface subsidence characteristics of Puning city. *Bulletin of Surveying and Mapping* **2021,** (6), 83-88.
13. Wang, N.; Xu, S.; Zhou, J., Analysis of land subsidence in coal mining area based on DInSAR technology. *The Chinese Journal of Geological Hazard and Control* **2016,** *27* (2), 110-114.
14. Dong, J.; Li, X.; Mei, Y.; Liu, S., D-InSAR monitoring of site stability for surface substation above old mine goaf. *Journal of Mining & Safety Engineering* **2022,** *39* (1), 62-71.
15. Liu, Z.-g.; Bian, Z.-f.; Lei, S.-g.; Liu, D.-l.; Sowter, A., Evaluation of PS-DInSAR technology for subsidence monitoring caused by repeated mining in mountainous area. *Transactions of Nonferrous Metals Society of China* **2014,** *24* (10), 3309-3315. http://dx.doi.org/10.1016/s1003-6326(14)63471-3
16. Liu, X.; Xing, X.; Wen, D.; Chen, L.; Yuan, Z.; Liu, B.; Tan, J., Mining-Induced Time-Series Deformation Investigation Based on SBAS-InSAR Technique: A Case Study of Drilling Water Solution Rock Salt Mine. *Sensors* **2019,** *19* (24). http://dx.doi.org/10.3390/s19245511
17. Yao, J.; Yao, X.; Chen, J.; Li, L.; Ren, K.; Liu, X., A study of deformation mode and formation mechanism of a bedding landslide induced by mining of gently inclined coal seam based on InSAR technology. *Hydrogeology & Engineering Geology* **2020,** *47* (3), 135-146.
18. Du, D.; Liu, H.; Zhou, J.; Zhang, J.; Miao, J.; Li, Y.; Cao, X.; Ye, M., Study of the characteristics and influencing factors of land subsidence in the Tongzhou district of Beijing. *Acta Geologica Sinica* **2022,** *96* (2), 712-725.
19. Yang, W.; He, Y.; Zhang, L.; Wang, W.; Chen, Y.; Chen, Y., InSAR monitoring of 3D surface deformation in Jinchuan mining area, Gansu Province. *Remote Sensing for Natural Resources* **2022,** *34* (1), 177-188.
20. Huang, W.; Song, T.; Li, H.; Liu, Y.; Hou, T.; Gao, M.; Zheng, Y., Design of Key Parameters for Strip-Filling Structures Using Cemented Gangue in Goaf-A Case Study. *Sustainability* **2023,** *15* (6). http://dx.doi.org/10.3390/su15064698
21. Zhu, X. J.; Guo, G. L.; Liu, H.; Chen, T.; Yang, X. Y., Experimental research on strata movement characteristics of backfill-strip mining using similar material modeling. *Bulletin of Engineering Geology and the Environment* **2019,** *78* (4), 2151-2167. http://dx.doi.org/10.1007/s10064-018-1301-y
22. Piao, C. D.; Wang, D.; Kang, H.; He, H.; Zhao, C. Q.; Liu, W. Y., Model test study on overburden settlement law in coal seam backfill mining based on fiber Bragg grating technology. *Arabian Journal of Geosciences* **2019,** *12* (13). http://dx.doi.org/10.1007/s12517-019-4564-0
23. Li, X. B.; Wang, D. Y.; Li, C. J.; Liu, Z. X., Numerical Simulation of Surface Subsidence and Backfill Material Movement Induced by Underground Mining. *Advances in Civil Engineering* **2019,** *2019*. http://dx.doi.org/10.1155/2019/2724370
24. Xiao, B.; Zhao, J.; Li, D.; Zhao, Z.; Xi, W.; Zhou, D., The Monitoring and Analysis of Land Subsidence in Kunming (China) Supported by Time Series InSAR. *Sustainability* **2022,** *14* (19). http://dx.doi.org/10.3390/su141912387
25. Li, Y.-x.; Yang, K.-m.; Zhang, J.-h.; Hou, Z.-x.; Wang, S.; Ding, X.-m., Research on time series InSAR monitoring method for multiple types of surface deformation in mining area. *Natural Hazards* **2022,** *114* (3), 2479-2508. http://dx.doi.org/10.1007/s11069-022-05476-8

26. Yang, Y.; Yang, W.; Peng, S.; Liu, J.; Zhang, T.; Shan, H., Land deformation monitoring in the Taiyuan area based on PS-InSAR. *Environmental Monitoring and Assessment* **2022,** *194* (9). http://dx.doi.org/10.1007/s10661-022-10311-5
27. Zhao, X.; Zhu, Q., Analysis of the surface subsidence induced by sublevel caving based on GPS monitoring and numerical simulation. *Natural Hazards* **2020,** *103* (3), 3063-3083. http://dx.doi.org/10.1007/s11069-020-04119-0
28. Sun, Y.; Zuo, J.; Karakus, M.; Liu, L.; Zhou, H.; Yu, M., A New Theoretical Method to Predict Strata Movement and Surface Subsidence due to Inclined Coal Seam Mining. *Rock Mechanics and Rock Engineering* **2021,** *54* (6), 2723-2740. http://dx.doi.org/10.1007/s00603-021-02424-z
29. Gu, W.; Chen, L.; Xu, D., Research on the Overburden Movement Law of Thick Coal Seam Without-Support Gangue-Filling Mining. *Minerals* **2023,** *13* (1). http://dx.doi.org/10.3390/min13010053
30. Luan, Y.; Dong, Y.; Ma, Y.; Weng, L., Surface and New Building Deformation Analysis of Deep Well Strip Mining. *Advances in Materials Science and Engineering* **2020,** *2020*. http://dx.doi.org/10.1155/2020/8727956
31. Guan, S.; Li, S.; Jin, C.; Liu, D., Study on Overlying Strata Movement Law in Backfill Mining of Gently Inclined Medium Thick Orebody. *Journal of Northeastern University. Natural Science* **2019,** *40* (11), 1630-1635.
32. Jia, L., Experimental study on failure characteristics of strata with different filling rates in longwall filling mining. *Coal Science and Technology* **2019,** *47* (9), 197-202.
33. Liu, Y.-F.; Wu, X.-H.; Zhu, T.; Wang, X.-J.; Zhang, G.-Y.; Wang, Z.-G., Influence of Mechanical Properties of Filling Paste on Overlying Strata Movement and Surface Settlement. *Shock and Vibration* **2022,** *2022*. http://dx.doi.org/10.1155/2022/4687200
34. Guo, K.; Guo, G.; Li, H.; Wang, C.; Gong, Y., Strata movement and surface subsidence prediction model of deep backfilling mining. *Energy Sources Part a-Recovery Utilization and Environmental Effects* **2020**. http://dx.doi.org/10.1080/15567036.2020.1838002
35. Chang, Q.; Yao, X.; Leng, Q.; Cheng, H.; Wu, F.; Zhou, H.; Sun, Y., Strata Movement of the Thick Loose Layer under Strip-Filling Mining Method: A Case Study. *Applied Sciences-Basel* **2021,** *11* (24). http://dx.doi.org/10.3390/app112411717
36. Zhang, G.; Wang, Z.; Guo, G.; Wei, W.; Wang, F.; Zhong, L.; Gong, Y., Study on Regional Strata Movement during Deep Mining of Erdos Coal Field and Its Control. *International Journal of Environmental Research and Public Health* **2022,** *19* (22). http://dx.doi.org/10.3390/ijerph192214902
37. Lv, W.; Wu, Y.; Wu, Y.; Xie, P.; Tan, Y.; Li, S., Movement deformation characteristics of overlying stratum in paste composite filling stope. *Energy Exploration & Exploitation* **2023,** *41* (3), 994-1014. http://dx.doi.org/10.1177/01445987231157126
38. 周钰博. 充填开采覆岩连续移动变形规律及沉陷预测研究. 博士, 中国矿业大学(北京), 2021.
39. 曹文杰. 大倾角煤层矸石局部充填覆岩运移规律研究. 硕士, 西安科技大学, 2021.
40. 刘茂福. 大倾角煤层局部充填长壁开采覆岩运移规律研究. 硕士, 西安科技大学, 2018.
41. Zhang, G. J.; Wang, Z. Y.; Guo, G. L.; Wei, W.; Wang, F. G.; Zhong, L. L.; Gong, Y. Q., Study on Regional Strata Movement during Deep Mining of Erdos Coal Field and Its Control. *International Journal of Environmental Research and Public Health* **2022,** *19* (22). http://dx.doi.org/10.3390/ijerph192214902
42. Luan, Y. Z.; Dong, Y.; Ma, Y. H.; Weng, L. Y., Surface and New Building Deformation Analysis of Deep Well Strip Mining. *Advances in Materials Science and Engineering* **2020,** *2020*. http://dx.doi.org/10.1155/2020/8727956